

Fibrin affects short-term in vitro human mesenchymal stromal cell responses to magneto-active fibre networks

Rose L. Spear^{1a}, Antonia Symeonidou^{1b}, Jeremy N. Skepper^{2c}, Roger A. Brooks^{3d}
and Athina E. Markaki^{*1}

¹*Department of Engineering, University of Cambridge, Trumpington Street, Cambridge, CB2 1PZ, UK*

²*Department of Physiology, University of Cambridge, Downing Street, Cambridge, CB2 3DY, UK*

³*Division of Trauma & Orthopaedic Surgery, Addenbrooke's Hospital, Hills Road, Cambridge, CB2 2QQ, UK*

(Received June 18, 2015, Revised September 11, 2015, Accepted September 14, 2015)

Abstract. Successful integration of cementless femoral stems using porous surfaces relies on effective peri-implant bone healing to secure the bone-implant interface. The initial stages of the healing process involve protein adsorption, fibrin clot formation and cell osteoconduction onto the implant surface. Modelling this process in vitro, the current work considered the effect of fibrin deposition on the responses of human mesenchymal stromal cells cultured on ferritic fibre networks intended for magneto-mechanical actuation of in-growing bone tissue. The underlying hypothesis for the study was that fibrin deposition would support early stromal cell attachment and physiological functions within the optimal regions for strain transmission to the cells in the fibre networks. Highly porous fibre networks composed of 444 ferritic stainless steel were selected due to their ability to support human osteoblasts and mesenchymal stromal cells without inducing untoward inflammatory responses in vitro. Cell attachment, proliferation, metabolic activity, differentiation and penetration into the ferritic fibre networks were examined for one week. For all fibrin-containing samples, cells were observed on and between the metal fibres, supported by the deposited fibrin, while cells on fibrin-free fibre networks (control surface) attached only onto fibre surfaces and junctions. Initial cell attachment, measured by analysis of deoxyribonucleic acid, increased significantly with increasing fibrinogen concentration within the physiological range. Despite higher cell numbers on fibrin-containing samples, similar metabolic activities to control surfaces were observed, which significantly increased for all samples over the duration of the study. It is concluded that fibrin deposition can support the early attachment of viable mesenchymal stromal cells within the inter-fibre spaces of fibre networks intended for magneto-mechanical strain transduction to in-growing cells.

Keywords: human mesenchymal stromal cells; fibrin; fibre networks; ferritic stainless steel; porous coatings

*Corresponding author, Ph.D., E-mail: am253@cam.ac.uk

^aPh.D., E-mail: rs489@cam.ac.uk

^bPh.D. student, E-mail: as2163@cam.ac.uk

^cPh.D., E-mail: jns1000@cam.ac.uk

^dPh.D., E-mail: rb10003@cam.ac.uk

1. Introduction

Cementless femoral stems using porous surfaces have gained widespread clinical acceptance for total joint arthroplasty in young, active patients (Nilsson *et al.* 2006). Secure bonding of these implants depends primarily upon the material-bone interface and effective peri-implant bone healing (Kuzyk and Schemitsch 2011). The first stage of the healing process involves protein adsorption onto the material surface, followed by fibrin clot formation and infiltration of cells, including pericytes, endothelial cells and human mesenchymal stromal cells (Kuzyk and Schemitsch 2011). An innovative approach to achieve enhanced peri-implant bone healing and in-growth in cementless implants involves magneto-mechanical actuation of porous surface layers made of bonded ferromagnetic fibres. Using an external magnetic field of around 1 Tesla (a field lower than those employed for diagnostic purposes), therapeutic levels of strain can be applied to in-growing bone as the fibre network deforms elastically in response to the applied field (Markaki and Clyne 2004, Markaki and Clyne 2005). A highly porous network made of bonded ferritic stainless steel fibres has been developed as a model for magneto-mechanical stimulation of in-growing cells and tissue (Malheiro *et al.* 2013, Spear *et al.* 2013, Markaki and Justin 2014, Neelakantan *et al.* 2014). A series of in vitro studies have evaluated the suitability of 444 ferritic stainless steel for biomedical applications (Malheiro *et al.* 2011, Malheiro *et al.* 2013, Spear *et al.* 2013, Symeonidou *et al.* 2013, Spear *et al.* 2015). Specifically, these materials support the osteogenic differentiation of human osteoblasts (Malheiro *et al.* 2013) and mesenchymal stromal cells (Symeonidou *et al.* 2013) into fully mature osteoblasts capable of mineral deposition. Furthermore, 444 ferritic stainless steel in the form of fully dense (2D) (Malheiro *et al.* 2011) and high porous fibre networks (3D) (Spear *et al.* 2013) surfaces, support monocyte cultures without inducing untoward cytotoxic or inflammatory responses. However, all of these studies have demonstrated that, at early time points, cells attach primarily onto the fibre surfaces and junctions. Depending on the initial cell concentration, filling the inter-fibre spaces can take several weeks. As the inter-fibre region affords the optimal position for transmission of strain to in-growing cells, it would be advantageous to promote cell attachment within this region at early time points.

Protein deposition during early stages of peri-implant bone healing may provide the necessary support for cells within the inter-fibre spaces, facilitating the transduction of strain to cells within the networks. Following implantation, extracellular matrix proteins and plasma proteins adsorb onto a prosthesis surface (Kuzyk and Schemitsch 2011). One of these plasma proteins is fibrin, which forms after enzymatic lysis of fibrinogen by thrombin and contributes to haemostasis (Doolittle 1984, Mosesson *et al.* 2001, Mosesson 2005). Physiological concentrations of fibrinogen range from 1.5 to 5 g L⁻¹ (Giddings and Bloom 1971, Arneson 1976, Kratz *et al.* 2004), but higher concentrations have been used extensively in clinical and tissue engineering applications (Silverman *et al.* 1999, Currie *et al.* 2001, Jackson 2001, Wong *et al.* 2003, Yamada *et al.* 2003, Eyrich *et al.* 2007, Lei *et al.* 2009). The majority of these applications use fibrinogen concentrations above physiological plasma levels (Silverman *et al.* 1999, Currie *et al.* 2001, Jackson 2001, Eyrich *et al.* 2007). Tissue engineering and cell delivery applications have used concentrations between 5 and 50 g L⁻¹ (Gorodetsky *et al.* 1999, Cox *et al.* 2004, Ho *et al.* 2006, Eyrich *et al.* 2007), while higher concentrations of 50 to 115 g L⁻¹ have been used for clinical sealants (Jackson 2001).

Studies concerning the effects of fibrinogen concentration on cell responses typically focus on supra-physiological concentrations (Cox *et al.* 2004, Ho *et al.* 2006, Barsotti *et al.* 2011). Recent work (Vavken *et al.* 2011, Colley *et al.* 2012, Spear *et al.* 2015) with human osteoblasts

contributed to the few studies elucidating the role of fibrin deposition from physiological conditions on cellular responses to porous implant surfaces. Previous work has demonstrated increased cell attachment without a corresponding increase in cell metabolic activity as a function of fibrinogen concentration (Spear *et al.* 2015), supporting similar reports of this behaviour in physiological ranges (Cox *et al.* 2004, Ho *et al.* 2006, Vavken *et al.* 2011).

Human mesenchymal stromal cells are among the first cells to attach to an implant surface and have the capacity to develop into mineralising osteoblasts during peri-implant bone healing (Kuzyk and Schemitsch 2011). Several chemical (Caplan 1991, Pittenger *et al.* 1999) and physical factors (Guilak *et al.* 2009, Clause *et al.* 2010) have been shown to influence the differentiation of mesenchymal stromal cells (Clause *et al.* 2010). Specifically, osteogenic differentiation can be induced by the addition of several chemical factors, including ascorbic acid, dexamethasone and β -glycerophosphate (Caplan 1991, Pittenger *et al.* 1999) or mechanical cues, such as stiffness (Dominici *et al.* 2006, Engler *et al.* 2006). This ability to direct mesenchymal stromal cell development through specific physical and chemical conditions coupled with their potential for clinical and tissue engineering applications (Lalu *et al.* 2012, Zaher *et al.* 2014) continues to stimulate ongoing research into these cells.

The present work considers the effects of physiological fibrin deposition on early-stage responses of human mesenchymal stromal cells cultured in vitro within porous ferromagnetic fibre networks. Cell attachment, proliferation and metabolic activity were examined for one week following fibrin deposition.

2. Materials and methods

2.1 Stainless steel fibre networks

Fibre network mats (Nikko Techno Ltd, Japan) were made from AISI 444, a ferritic stainless steel. Typical fibre distributions and surface morphologies have been published previously (Spear *et al.* 2015). Briefly, the fibre networks were manufactured by shaving 80 μm fibres off a 100 μm thick sheet, hence they exhibit a rectangular fibre cross-section. The fibres lie in-plane, occupy $16\pm 1\%$ of the network volume and are bonded together at cross-over points by solid-state sintering. The materials were supplied as 1 mm thick flat mats and cut into ~ 9.5 mm diameter discs using a punch press. For cell culture, the discs were ultrasonically cleaned for 15 min in a sequence of acetone, ethanol and distilled water. Samples were dried at 60°C for 1 h and then sterilised by dry heat at 160°C for 2 h.

2.2 Human mesenchymal stromal cells

All cell culture reagents were obtained from Invitrogen (Paisley, UK) and all other chemicals from Sigma (Poole, UK) except where indicated. Human mesenchymal stromal cells, hMSCs (Lonza, PT-2501), were maintained in Lonza hMSC growth medium (PT-3001). Cultures were incubated at 37°C in a humidified atmosphere containing 5% CO₂ and medium was replaced every 3-4 days. After 6 days, cells were detached from culture flasks using 0.25% trypsin-EDTA for further subculture or seeding. Cells from the 5th passage were used for all experiments.

2.3 Fibrin deposition and cell seeding

Thrombin was prepared as a 0.025 U/ μ L solution in DPBS and frozen at -20°C until seeding. Before seeding, the fibre networks were wetted for 1 h with the growth medium. After removing excess medium under aseptic conditions, samples were placed on a sterile, hydrophobic polytetrafluoroethylene (PTFE) filter to prevent droplet spreading. The fibrinogen solution was freshly prepared in sterile vials to each concentration (0, 3, 5 or 10 g L⁻¹) using growth medium (pre-warmed to 37°C) and maintained at 37°C on a heated stage. A 50 μ L droplet of fibrinogen solution (37°C) was added to each sample. A 50 μ L droplet of thrombin (0.1 U/mg fibrinogen, 37°C) was then added and the solutions were mixed by pipetting. The samples were incubated for 1 h at 37°C to allow for fibrinogen lysis and fibrin deposition in the networks. Cells were added to fibre networks (5×10^4 cells per network) in a 100 μ L droplet of growth medium and mixed gently by pipetting. The samples were incubated for 4 h at 37°C to allow for cell attachment. After this period, the samples were each transferred to individual wells of a 24 well culture plate (non-treated polystyrene) and 1 mL of pre-warmed growth medium (37°C) was added to each well.

2.4 Fibrin and cell morphology

Scanning electron, fluorescence and confocal laser scanning microscopy were employed to investigate fibrin and cell attachment on the fibre networks. For scanning electron microscopy (SEM), samples were washed twice with DPBS, fixed in 2.5% (v/v) glutaraldehyde solution in DPBS for 1 h at $4-6^{\circ}\text{C}$, washed thrice with DPBS and dehydrated in graded series of ethanol (70, 85, 95 and 100%). Samples were dried using hexamethyldisilazane, mounted on aluminium stubs with carbon tape, gold coated (2.4 kV, 90s) and observed under a Zeiss Evo MA 15 scanning electron microscope.

For freeze cracking, samples were washed twice with DPBS, fixed in 2.5% (v/v) glutaraldehyde solution in DPBS for 1 h at $4-6^{\circ}\text{C}$ and washed thrice with DPBS. Samples were then immersed in liquid nitrogen and placed in a custom-holder that positioned each sample end-on. Samples were fractured in half by sharp application of a razor.

For fluorescence microscopy, samples were washed once with DPBS, fixed with 4% (w/v) paraformaldehyde in PBS (15 min, 20°C , Affymetrix, High Wycombe, UK) and washed thrice with DPBS. They were incubated with 2% (w/v) goat serum albumin (GSA) in DPBS (30 min, 20°C) to block non-specific binding and then washed twice with DPBS. For fibrin imaging, samples were incubated with a monoclonal anti-fibrinogen raised in mouse (Sigma, 24 h, $4-6^{\circ}\text{C}$), washed thrice with 0.05% tween-20 in DPBS and incubated with a 1:100 dilution in DPBS of goat anti-mouse antibody conjugated to AlexaFluor594 (1 h, $4-6^{\circ}\text{C}$, foil-wrapped) and washed twice with 0.05% tween-20 in DPBS, mounted with gold anti-fade mountant and imaged using a Zeiss Axio Observer Z1 with an ORCA-flash 4.0 digital CMOS.

For confocal laser scanning microscopy (CLSM), samples were washed once with DPBS, fixed with 4% (w/v) paraformaldehyde in PBS (15 min, 20°C , Affymetrix, High Wycombe, UK) and washed thrice with DPBS. They were incubated with 2% (w/v) GSA in DPBS (30 min, 20°C) to block non-specific binding and then washed twice with DPBS. The samples were permeabilised at $4-6^{\circ}\text{C}$ for 10 min in pH 7.2 buffer composed of sucrose (10.3 g), sodium chloride (0.292 g), magnesium chloride (0.06 g), 4-(2-hydroxyethyl)-1-piperazineethanesulfonic acid (HEPES) buffer (0.476 g) and Triton-X (0.5 mL) in distilled water (100 mL). Subsequently, the samples were incubated with a 1:100 dilution in DPBS of AlexaFluor488-phalloidin conjugate (1 h, 20°C),

washed thrice with 0.05% tween-20 in DPBS, mounted with gold anti-fade mountant and imaged using a Leica DMIRE2 confocal microscope. Images were prepared as maximum projections of z-stacks using Fiji software.

2.5 Cell attachment and proliferation

Cell cultures were assayed for deoxyribonucleic acid (DNA) to give an indication of initial cell attachment and proliferation. After binding to nucleic acids, the proprietary CyQuant® fluorescent dye exhibits a fluorescent signal, which can be calibrated to cell number using a standard curve. The CyQuant® assay was used according to the manufacturer's instructions to determine cell number in triplicate at each time point. Briefly, the medium was removed and the samples were washed once with DPBS and frozen at -80°C until measurement. CyQuant® lysis solution containing ribonuclease (RNase) (1.35 kunitz units/mL) was added to each sample and the solution was shaken for 1 h. Aliquots were transferred in triplicate to a black 96-well microplate. CyQuant® dye was added to the cell lysate aliquots and DNA content was measured fluorimetrically (excitation 480 nm, emission 520 nm) on a Fluostar Optima multidetection microplate reader (BMG Labtech, Offenburg, Germany). A reference standard curve of known cell number versus fluorescence was prepared for each assay, using cell aliquots that were counted and frozen on the day of seeding and then stored at -80°C, in order to convert the measured fluorescence values into cell numbers.

2.6 Cell metabolic activity

The alamarBlue® assay (Serotec, Oxford, UK) measures proliferation and viability by quantification of intracellular metabolic activity. Intracellular metabolic activity results in the reduction of resazurin, the blue (non-fluorescent) cell permeable ingredient of alamarBlue® reagent, to resorufin, a compound that is red in colour and highly fluorescent (Lancaster and Fields 1996). Triplicate samples were incubated for 4 hours with fresh growth medium supplemented with 10% (v/v) alamarBlue® reagent. Following incubation, 100µL medium from each well was transferred in triplicate to a black 96-well microplate. Fluorescence (excitation 530 nm, emission 590 nm) was measured using the aforementioned reader. The percent reduction of alamarBlue® was calculated using Eq. (1)

$$\% \text{ reduction of alamarBlue®} = \frac{S_{AB}^x - S_{AB}^{control}}{S_{AB}^{100\% \text{ reduced}} - S_{AB}^{control}} \quad (1)$$

where S_{AB}^x was the alamarBlue® fluorescence signal of the sample at day x , $S_{AB}^{100\% \text{ reduced}}$ is the signal of the 100% reduced form of alamarBlue® and $S_{AB}^{control}$ is the signal from the control solution: the culture medium supplemented with 10% alamarBlue® dye. The 100% reduced form of alamarBlue® was produced by autoclaving the control solution at 121°C for 15 min.

2.7 hMSC phenotype and differentiation

Cells were cultured in standard cell culture flasks (Greiner Bio-one) in growth medium for 6 days, trypsinised and collected by centrifugation (300 g, 5 min, RT). They were re-suspended in 50

μL staining buffer and incubated for 30 min (4-6°C) with individual antibodies (Table 1). Following incubation, cells were washed with staining buffer, centrifuged (300 g, 5 min, 4°C), fixed in BD Cytotfix/Cytoperm buffer (30 min, 4-6°C) (BD Pharmingen Biosciences), centrifuged (300 g, 5 min, 4°C) and frozen in 10% dimethyl-sulfoxide in heat-inactivated FBS using a cryogenic freezing container (-80°C). Samples were quickly thawed on the day of analysis in a 37°C water bath, washed with staining buffer, refixed in BD Cytotfix/Cytoperm buffer (5 min, 4-6°C) and re-suspended in staining buffer for analysis. Acquisition and analysis was performed on a Beckman Coulter Cyan ADP using Summit Software 4.3 (Fluorochrome: laser line, emission filter; PE: 488 nm; 574/25; PerCP-CyTM5.5: 488 nm, 680/30; APC: 642 nm, 665/20). Data analysis was performed using Flow Jo software. 5,000 cells were gated for the positive hMSC markers and corresponding isotypes, while 10,000 cells were gated for negative hMSC marker and corresponding isotype.

Osteogenic differentiation was characterised by alkaline phosphatase (ALP) activity. Duplicate aliquots of 50 μL were removed from each sample lysate, prepared as for the CyQuant® assay, and mixed with 50 μL of ALP Assay buffer containing 6,8-difluoro-4-methylumbelliferyl phosphate (DiFMUP). Triplicate samples were incubated (37°C, 15 min) to produce the fluorescent compound 6,8-difluoro-7-hydroxy-4-methylcoumarin (DiFMU). ALP activity was measured fluorometrically (excitation 358 nm, emission 455 nm), using the aforementioned reader. The emission intensity units of the signal were converted to the quantity of DiFMU per 10^3 cells using a DiFMU standard curve.

2.8 Statistical analysis

Averages of three independent experiments, with three tested samples per fibrin concentration, were expressed as the arithmetic mean \pm standard deviation (SD). Data were analysed for homogeneity of variance with Levene's test. Data with homogenous variance were analysed for statistical significance by two-way analysis of variance (ANOVA), followed by Tukey's post-hoc test for multiple comparisons. Differences were considered statistically significant at p values of <0.05 ($n=3$).

3. Results

3.1 Fibrin deposition

444 stainless steel fibre networks following the deposition of fibrin through the lysis of fibrinogen by thrombin are presented in Fig. 1. Figs. 1(a)-(d) show high magnification SEM images of a selected region of the top surface. A control surface without fibrin is shown in Fig. 1(a). In Figs. 1(b)-(d), the deposited fibrin consisted of nanoscale fibres fused together with, qualitatively, smaller inter-fibre spaces in supra-physiological concentrations than physiological concentrations. Figs. 1(e)-(h) show fluorescence images of the top surface of the fibre networks after fibrin deposition. It can be seen that fibrin (stained red with AlexaFluor594) covered completely the top surface of the fibre networks for all fibrin-containing samples (Figs. 1(f)-(h)). Fibrin was also observed on the bottom surface of the samples, though the coverage was incomplete and varied between the fibrinogen concentrations (Figs. 1(j)-(l)).

3.2 hMSC phenotype

Flow cytometry data are presented as histograms in Figs. 2(a)-(d). The data shows that the cells expressed CD105, CD73 and CD90 and did not express CD14 prior to seeding on the scaffolds. The activity of alkaline phosphatase, an indicator of early osteoblast differentiation, is presented for hMSCs in Fig. 2(e). Similar low levels of ALP activity were measured for all samples throughout the duration of the study.

3.3. Cell attachment, proliferation and metabolic activity

Fig. 3(a) presents the number of hMSCs measured by CyQuant® on the samples following 1, 3, and 7 days of incubation. After 1 day of culture, significantly higher numbers of hMSCs were measured for the highest concentrations of fibrin (5 and 10 g L⁻¹) compared with the control networks without fibrin. However, cell numbers on all samples (with or without fibrin) remained statistically similar for days 3 and 7 of the study. The number of cells attached to each sample is presented as a percent of the initial seeding concentration in Fig. 3(b). The results show a positive correlation between fibrin concentration and percent of hMSCs seeded within the physiological

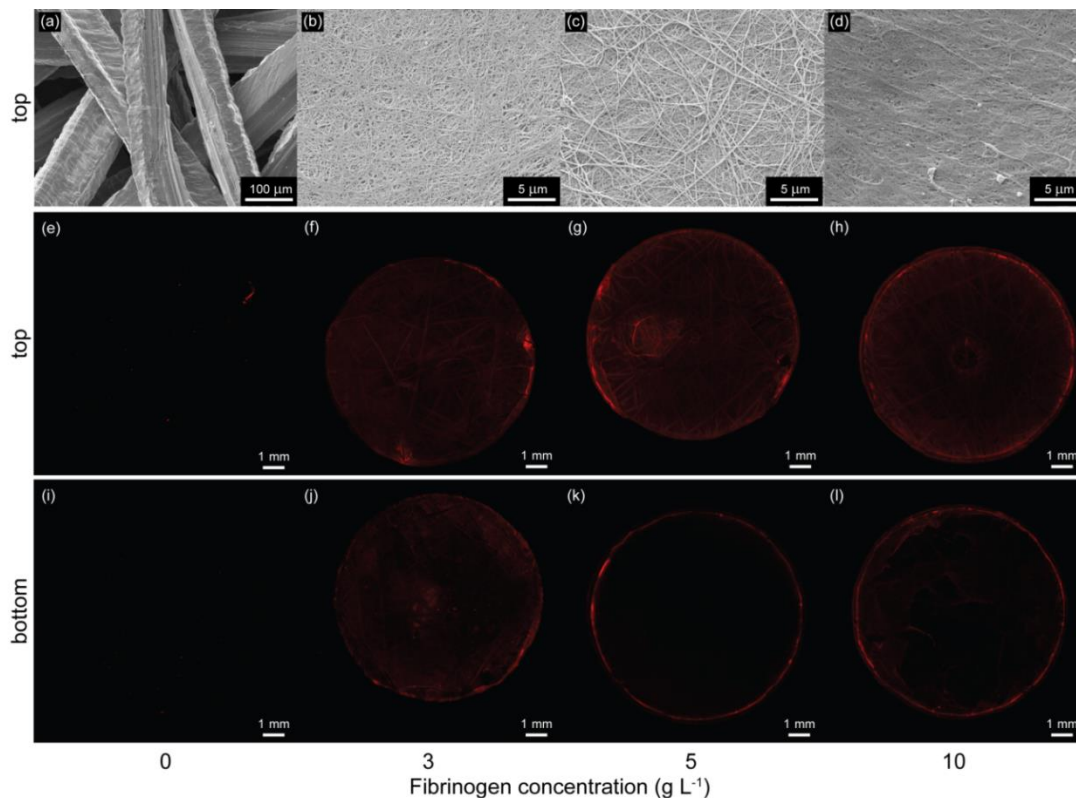


Fig. 1 SEM images showing the top view of 444 ferritic fibre networks following fibrin deposition from (a) 0 g·L⁻¹, (b) 3 g·L⁻¹, (c) 5 g·L⁻¹ and (d) 10 g·L⁻¹ fibrinogen solutions. Fluorescence images of 444 ferritic fibre networks following fibrin deposition from (e, i) 0 g·L⁻¹, (f, j) 3 g·L⁻¹, (g, k) 5 g·L⁻¹ and (h, l) 10 g·L⁻¹ fibrinogen solutions, showing (e)-(h) top and (i)-(j) bottom surfaces

range; the seeding efficiency on day 1 increased as the concentration of fibrin increased. Fig. 3(c) indicates the metabolic activity of hMSCs as measured by the reduction of alamarBlue®. The hMSCs had similar metabolic activities on all samples. The metabolic activity for all samples significantly increased for all samples over the duration of the study.

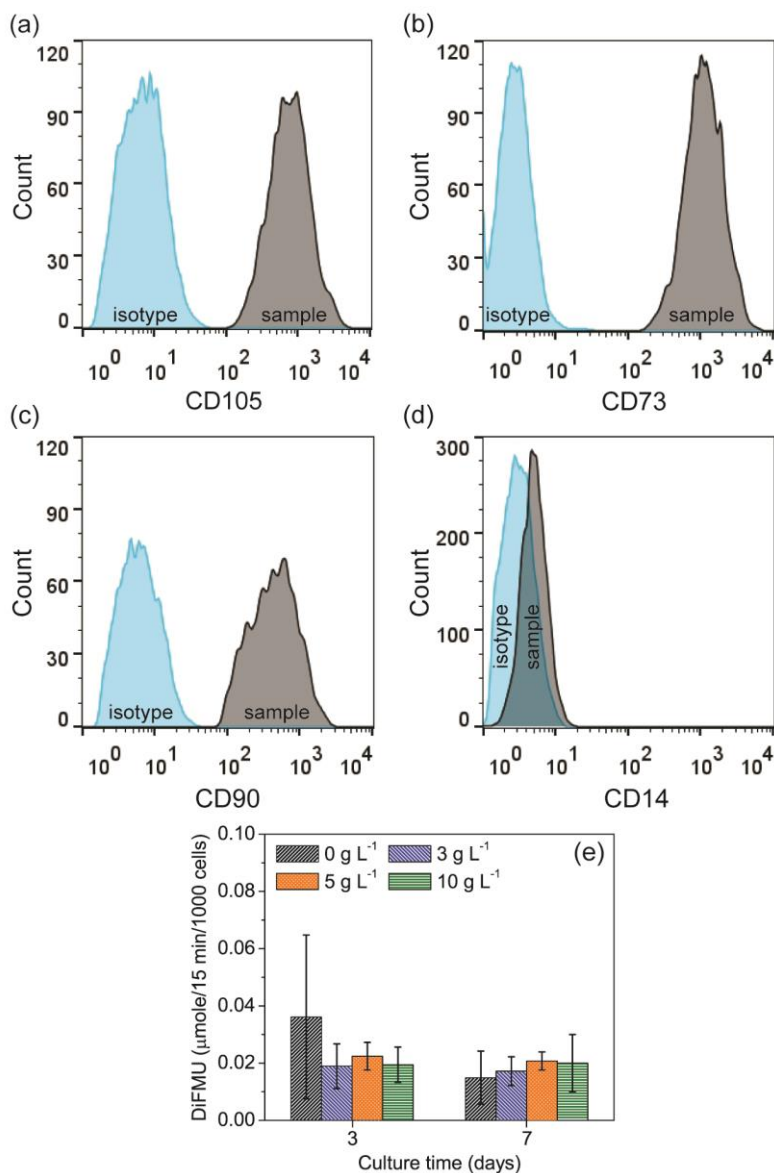


Fig. 2 Histograms showing flow cytometry data for hMSC cells stained for positive hMSC markers: (a) CD105-PE, (b) CD73-APC and (c) CD90-PerCP-CyTM5.5 and the negative hMSC marker: (d) CD14. Histograms show isotype controls (blue) and samples (grey). (e) Alkaline phosphatase (ALP) activity of hMSCs after 3 and 7 days following fibrin deposition from 0, 3, 5 and 10 g L⁻¹ fibrinogen solutions. ALP activity is presented as the amount of DiFMU (μmoles) produced per 10³ cells after incubation at 37°C for 15 min

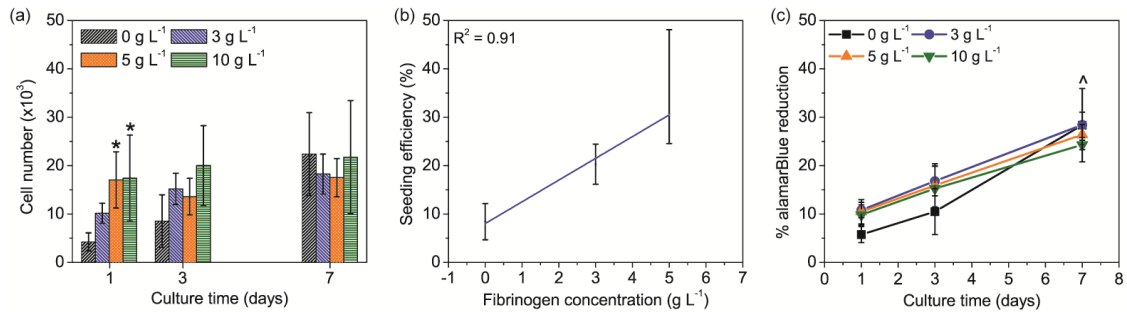


Fig. 3 (a) CyQuant[®] analysis for cell number as measured by DNA content, (b) seeding efficiency, presented as a percent of initial seeding concentration, as a function of fibrinogen concentration and (c) metabolic activity as measured by the alamarBlue[®] assay for HMSCs seeded onto fibre networks for 1, 3 and 7 days following fibrin deposition from 0, 3, 5 and 10 g L^{-1} fibrinogen solutions. Two-way ANOVA analysis was performed to test for statistical significance using Bonferroni post-hoc analysis (Mean \pm SD, $n=3$, $p<0.05$). * indicates significance with respect to control fibrinogen concentration (0 g L^{-1}). ^ indicates significance with respect to initial metabolic activity (day 1)

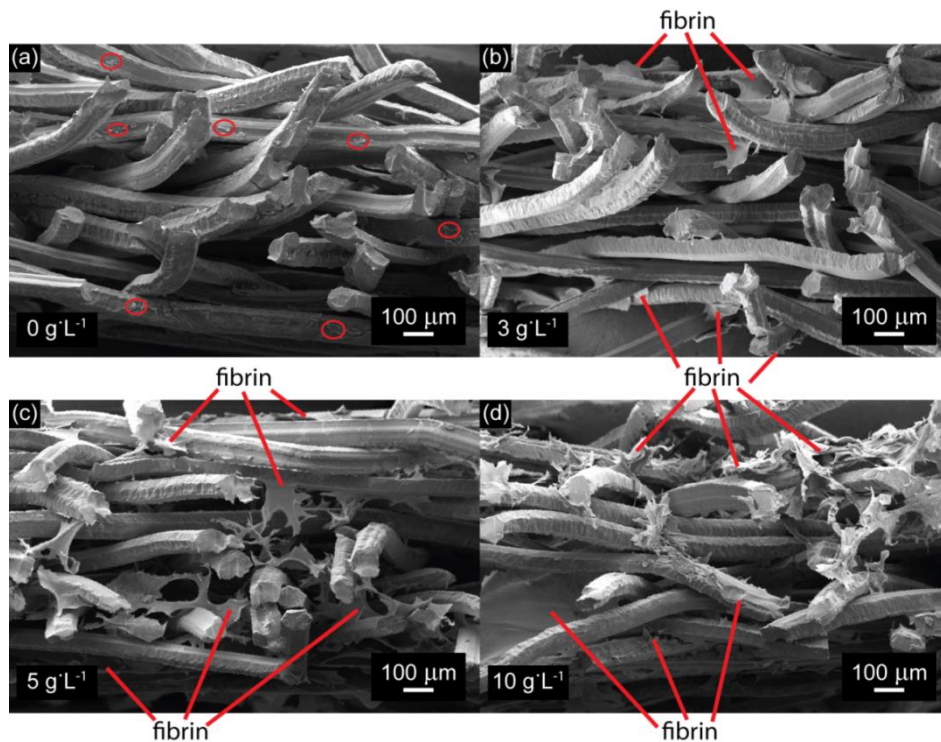


Fig. 4 SEM images showing cross-sectional view of stainless steel fibre networks following fibrin deposition from (a, e) 0 g L^{-1} , (b) 3 g L^{-1} , (c) 5 g L^{-1} and (d) 10 g L^{-1} fibrinogen solutions after 1 week of cell culture. Selected cells are circled in Fig. (a). Selected fibrin is identified by lines in Figs. (b)-(d)

3.4 Cell and fibrin penetration

SEM images of freeze-cracked sections of the fibre networks after 7 days of cell culture with

hMSCs are shown in Fig. 4. Fig. 4(a) shows that cells attached onto the fibre surfaces in the control fibre networks (without fibrin). In fibrin-coated networks, fibrin was observed throughout the network depth as shown in Figs. 4(b)-(d). Qualitative analysis of these images showed that the amount of deposited fibrin decreased as the fibrinogen concentration decreased.

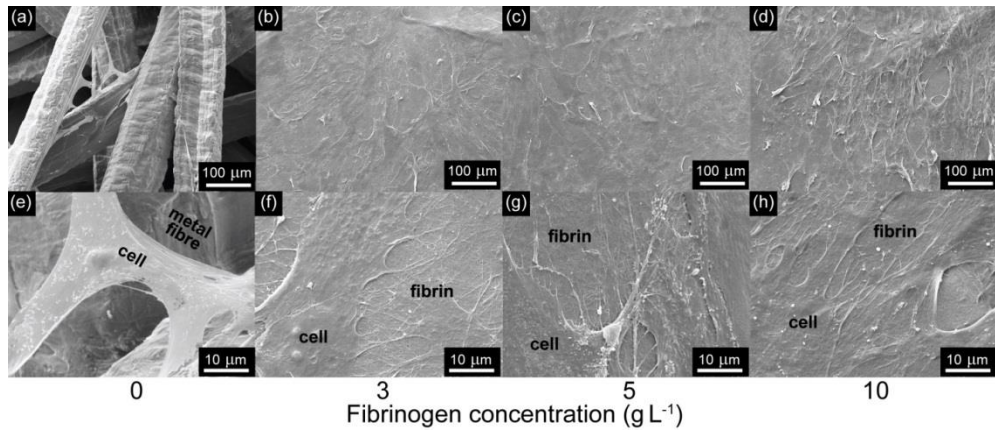


Fig. 5 SEM images showing (a)-(d) low and (e)-(h) high magnification images of HMSCs cultured on 444 stainless steel fibre networks with (a, e) 0 g·L⁻¹, (b, f) 3 g·L⁻¹, (c, g) 5 g·L⁻¹ and (d, h) 10 g·L⁻¹ fibrin after 1 day of culture

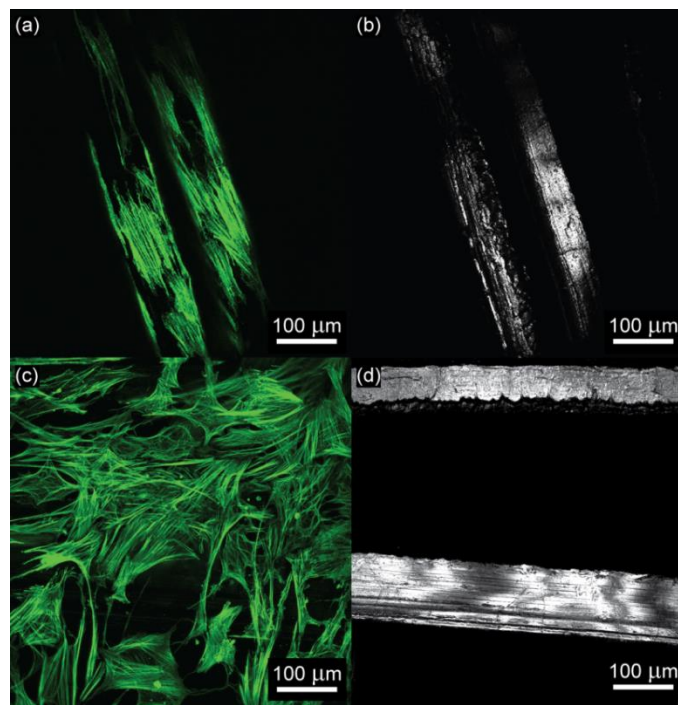


Fig. 6 CLSM images of HMSCs cultured for seven days on 444 stainless steel fibre networks with (a,b) 0 g·L⁻¹ fibrin and (c,d) 3 g·L⁻¹ fibrin. (a,c) Actin filaments (green) were stained with AlexaFluor488[®]-conjugated phalloidin. (b,d) Fibres (grey) were imaged through reflectance

3.5 Cell and fibrin morphology

SEM images of the top surface of the fibre networks following fibrin deposition and cell seeding of hMSCs are shown in Fig. 5. Cells on the control samples without fibrin were observed only on the metal fibres and bridging junctions between fibres as shown in Fig. 5(a) and 5(e). In contrast, extensive attachment of fibrin and cells over the surface of the fibre networks was observed in fibrin-coated networks (Figs. 5(b)-(d)). Cells, attached to the fibrin-coated networks, showed extensive spreading and numbers of cytoplasmic projections as shown in Figs. 5(f)-(h). The nanoscale threadlike morphology of the fibrin nanofibres was also visible in Figs. 5(f)-(h).

SEM observations of cell attachment over the surface of the fibrin-coated samples were confirmed by fluorescence images (Fig. 6). The fluorescence images of the control samples (without fibrin) shown in Figs. 6(a)-(b) confirmed the association of the cells solely with the metal fibres. In contrast, the fibrin-coated samples clearly showed cells attached in the inter-fibre spaces as well as on the fibre surfaces as shown in Figs. 6(c)-(d). After one week of culture, cells exhibited a well-defined arrangement of actin stress fibres on both fibrin-coated and control networks.

4. Discussion

In the current work, we have presented the first study concerning the effect of fibrin deposition on the early *in vitro* response of human mesenchymal stromal cells to porous fibre networks made of 444 ferritic stainless steel. These networks have been proposed for use as magneto-active layers on implants for stimulation of growth of in-growing bone by the application of an external magnetic field of around 1 Tesla. A schematic representation of this process is presented in Fig. 7, showing fibrin deposition, cell seeding and the deformation of the fibres upon application of an external magnetic field. It was hypothesized that fibrin would promote cell attachment within the inter-fibre spaces at early time points as compared to networks without fibrin. The fibre networks employed (Fig. 1(a)) have been fully characterised previously (Spear *et al.* 2015). They are produced by bonding together a set of rectangular fibres. The fibres are lying at low inclination angles to the horizontal and occupy about 16% of the volume.

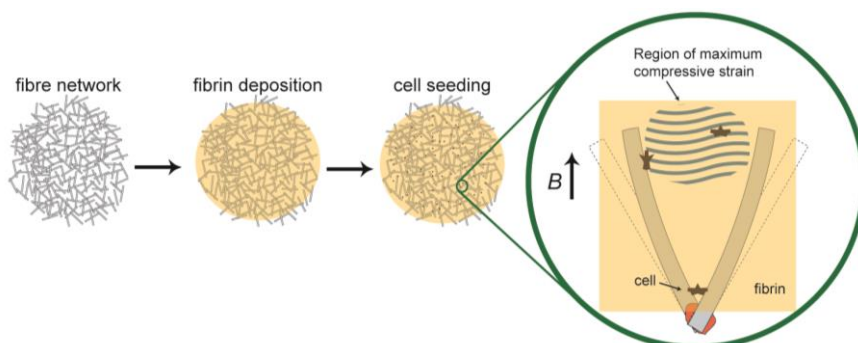


Fig. 7 A schematic representation of a ferromagnetic fibre network following fibrin deposition and cell seeding. The insert shows how a pair of bonded fibres will deflect when subjected to an external magnetic field B

The present study builds upon earlier work that demonstrated the ability of these networks to support human osteoblasts (Malheiro *et al.* 2013) and mesenchymal stromal cells (Symeonidou *et al.* 2013), without untoward inflammatory responses (Spear *et al.* 2013). The results further our recent work using fibrin to support human osteoblasts in these networks (Spear *et al.* 2015). The current work focuses on human mesenchymal stromal cells, a small multipotent cell population from bone marrow, which are involved in the response of bone following implantation (Kuzyk and Schemitsch 2011). Three minimal criteria were proposed in 2006 by the International Society for Cellular Therapy (ISCT) for the identification of multipotent mesenchymal marrow stromal cells *in vitro* (Dominici *et al.* 2006), including adherence to plastic, expression of CD105, CD73 and CD90 and absence of CD45, CD34, CD14 or CD11b, CD79 α or CD19 and HLA-DR surface molecules, and finally the capability to differentiate down osteogenic, adipogenic and chondrogenic lineages (Engler *et al.* 2006). In light of ongoing research, these criteria are continually being expanded and revised (Bianco *et al.* 2013); however, the ISCT definition provides the basis for identification of a specific expanded cell population *in vitro* that have been termed mesenchymal stromal cells. As shown in Fig. 2, the cells used in this study expressed the typical hMSC markers: CD105, CD73 and CD90 (Figs. 2(a)-(c)), but lacked expression of CD14 (Fig. 2(d)), which would be expressed by monocytes, macrophages and neutrophils. Additionally, the levels of alkaline phosphatase activity remained at a similar baseline level throughout the study duration (Fig. 2(e)) for all samples. The results provide evidence that the cells were multipotent marrow stromal cells prior to seeding and lacked a significant level of differentiation towards an osteogenic lineage for the duration of the study. This can be attributed to the absence of chemical factors that induce osteogenic differentiation, such as ascorbic acid, dexamethasone and β -glycerophosphate (Caplan 1991, Pittenger *et al.* 1999).

The design of the current studies was based on the initial stages of peri-implant bone healing *in vivo*, involving implantation, rupture of blood vessels, protein deposition, fibrin clotting and osteoconduction. In keeping with this model, fibrin was deposited prior to cell seeding using concentrations around the physiological range of 1.5 to 5 g L⁻¹ (Cox *et al.* 2004, Ho *et al.* 2006) with one supra-physiological concentration (10 g L⁻¹). The deposited fibrin was observed to consist of nanoscale fibres fused together with qualitatively smaller inter-fibre spaces for supra-physiological concentrations compared with physiological concentrations (Fig. 1(b)-(d)). The observation of decreased inter-fibre pores with higher fibrinogen concentrations agrees well with literature reports on fibrin deposition (Giddings and Bloom 1971, Spear *et al.* 2015). Since the envisaged prosthesis design would involve sintering the networks to the femoral stem, only one side of the networks was exposed to fibrin and cells during seeding. Due to this approach, the coverage of fibrin varied between the top and bottom surfaces. While fibrin covered the top surface of the networks, coverage on the bottom surface was incomplete and varied depending on fibrinogen concentration (Figs. 1(e)-(l)). SEM images of freeze-cracked samples (Fig. 4) provided further support for these observations. In these freeze-cracking images, the amount of fibrin was observed to increase with increasing fibrinogen concentration and decrease with network depth (Fig. 4). Both the fluorescence staining of fibrin (Fig. 1) and the freeze-cracking cross-sections (Fig. 4) demonstrated that fibrin was present within the samples throughout the duration of the study.

Cell attachment of hMSCs was observed over the surface of the networks and the fibrin in both fluorescence and SEM images (Figs. 5 and 6). Cells had spread morphologies with well-defined cytoplasmic projections on all samples. While attachment in control samples was restricted to the metal fibre surfaces and junctions, cells in fibrin-containing samples were observed both on and

between the fibres. For all concentrations, cell attachment was supported by fibrin within the inter-fibre spaces.

The short-term cellular behaviour of the hMSCs, in terms of attachment and metabolic activity, showed dependencies on fibrinogen concentration and culture time. Generally, the initial seeding efficiency was directly correlated with the fibrin concentration within physiological ranges, resulting in significant increases in initial cell attachment with increasing fibrin concentration (Figs. 3(a)-(b)). Supra-physiological and high physiological concentrations had similar attachment levels that were significantly higher than control samples. Despite this increased cell attachment, the cell populations had similar metabolic activity for all fibrinogen concentrations (Fig. 3(c)), indicating a lower metabolic activity per cell for supra-physiological concentrations. These results agreed with earlier results for human osteoblasts (Cox *et al.* 2004, Ho *et al.* 2006, Vavken *et al.* 2011, Spear *et al.* 2015). Increased fibrin deposition from physiological concentrations contributed to higher cell attachment as the fibrin supported the cells within the inter-fibre regions without a corresponding increase in metabolic activity.

5. Conclusions

The results of the current study demonstrate that deposition of fibrin following fibrinogen lysis by thrombin affects the attachment and metabolic activity of human mesenchymal stromal cells in porous ferritic stainless steel fibre networks. The deposition of fibrin provided support for cells between the metal fibres, within the region for strain transduction. Specific effects of the fibrin coatings depended upon protein concentration and culture time; however, general trends were observed independent of these factors. Generally, the seeding efficiency was directly correlated with the fibrin concentration within physiological ranges. Despite higher cell attachment, cells exhibited similar levels of metabolic activity at the various levels of fibrin deposition, indicating lower metabolic activities per cell for higher concentrations. These results demonstrate that physiologically relevant fibrin deposition can support the early attachment of viable stromal cells within the inter-fibre spaces of magneto-active networks intended for magneto-mechanical strain transduction to in-growing cells.

Acknowledgements

This research was supported by the European Research Council (Grant No. 240446). Financial support for RAB has been provided via the National Institute for Health Research (NIHR). RLS would like to thank Nigel Miller for assistance with the flow cytometry measurements.

References

- Arneson, D. (1976), "Quantitative-analysis of plasma fibrin monomer", *Thrombosis Res.*, **8**(1), 31-41.
- Barsotti, M.C., Magera, A., Armani, C., Chiellini, F., Felice, F., Dinucci, D., Piras, A.M., Minnocci, A., Solaro, R., Soldani, G., Balbarini, A. and Di Stefano, R. (2011), "Fibrin acts as biomimetic niche inducing both differentiation and stem cell marker expression of early human endothelial progenitor cells", *Cell Proliferation*, **44**(1), 33-48.
- Bianco, P., Cao, X., Frenette, P.S., Mao, J.J., Robey, P.G., Simmons, P.J. and Wang, C.Y. (2013), "The

- meaning, the sense and the significance: translating the science of mesenchymal stem cells into medicine”, *Nat. Med.*, **19**(1), 35-42.
- Caplan, A.I. (1991), “Mesenchymal stem cells”, *J. Orthop. Res.*, **9**(5), 641-650.
- Clause, K.C., Liu, L.J. and Tobita, K. (2010), “Directed stem cell differentiation: the role of physical forces”, *Cell Commun. Adhesion*, **17**(2), 48-54.
- Colley, H., McArthur, S.L., Stolzing, A. and Scutt, A. (2012), “Culture on fibrin matrices maintains the colony-forming capacity and osteoblastic differentiation of mesenchymal stem cells”, *Biomed. Mater.*, **7**(4), 045015.
- Cox, S., Cole, M. and Tawil, B. (2004), “Behavior of human dermal fibroblasts in three-dimensional fibrin clots: Dependence on fibrinogen and thrombin concentration”, *Tissue Eng.*, **10**(5-6), 942-954.
- Currie, L.J., Sharpe, J.R. and Martin, R. (2001), “The use of fibrin glue in skin grafts and tissue-engineered skin replacements: A review”, *Plastic Reconstruct. Surg.*, **108**(6), 1713-1726.
- Dominici, M., Le Blanc, K., Mueller, I., Slaper-Cortenbach, I., Marini, F.C., Krause, D.S., Deans, R.J., Keating, A., Prockop, D.J. and Horwitz, E.M. (2006), “Minimal criteria for defining multipotent mesenchymal stromal cells. The International Society for Cellular Therapy position statement”, *Cytother.*, **8**(4), 315-317.
- Doolittle, R.F. (1984), “Fibrinogen and fibrin”, *Ann. Rev. Biochem.*, **53**(1), 195-229.
- Engler, A.J., Sen, S., Sweeney, H.L. and Discher, D.E. (2006), “Matrix elasticity directs stem cell lineage specification”, *Cell*, **126**(4), 677-689.
- Eyrich, D., Brandl, F., Appel, B., Wiese, H., Maier, G., Wenzel, M., Staudenmaier, R., Goepferich, A. and Blunk, T. (2007), “Long-term stable fibrin gels for cartilage engineering”, *Biomater.*, **28**(1), 55-65.
- Giddings, J.C. and Bloom, A.L. (1971), “Study of 2 methods for estimating plasma fibrinogen and effect of epsilon aminocaproic acid and protamine”, *J. Clin. Pathol.*, **24**(5), 467-471.
- Gorodetsky, R., Clark, R.A.F., An, J.Q., Gailit, J., Levdansky, L., Vexler, A., Berman, E. and Marx, G. (1999), “Fibrin microbeads (FMB) as biodegradable carriers for culturing cells and for accelerating wound healing”, *J. Invest. Dermatol.*, **112**(6), 866-872.
- Guilak, F., Cohen, D.M., Estes, B.T., Gimple, J.M., Liedtke, W. and Chen, C.S. (2009), “Control of stem cell fate by physical interactions with the extracellular matrix”, *Cell Stem Cell*, **5**(1), 17-26.
- Ho, W., Tawil, B., Dunn, J.C.Y. and Wu, B.M. (2006), “The behavior of human mesenchymal stem cells in 3D fibrin clots: Dependence on fibrinogen concentration and clot structure”, *Tissue Eng.*, **12**(6), 1587-1595.
- Jackson, M.R. (2001), “Fibrin sealants in surgical practice: An overview”, *Am. J. Surg.*, **182**(2), S1-S7.
- Kratz, A., Ferraro, M., Sluss, P.M. and Lewandrowski, K.B. (2004), “Laboratory reference value”, *New England J. Med.*, **351**(15), 1548-1563.
- Kuzyk, P.R.T. and Schemitsch, E.H. (2011), “The basic science of peri-implant bone healing”, *Indian J. Orthop.*, **45**(2), 108-115.
- Lalu, M.M., McIntyre, L., Pugliese, C., Fergusson, D., Winston, B.W., Marshall, J.C., Granton, J., Stewart, D.J. and Canadian Critical Care Trials, G. (2012), “Safety of cell therapy with mesenchymal stromal cells (SafeCell): A systematic review and meta-analysis of clinical trials”, *PLoS ONE*, **7**(10), e47559.
- Lancaster, M.V. and Fields, R.D. (1996), *Antibiotic and cytotoxic drug susceptibility assays using resazurin and poisoning agents*, Alamar Biosciences Laboratory, Inc.: 2313.
- Lei, P., Padmashali, R.M. and Andreadis, S.T. (2009), “Cell-controlled and spatially arrayed gene delivery from fibrin hydrogels”, *Biomater.*, **30**(22), 3790-3799.
- Malheiro, V.N., Skepper, J.N., Brooks, R.A. and Markaki, A.E. (2013), “In vitro osteoblast response to ferritic stainless steel fiber networks for magneto-active layers on implants”, *J. Biomed. Mater. Res. Part A*, **101A**(6), 1588-1598.
- Malheiro, V.N., Spear, R.L., Brooks, R.A. and Markaki, A.E. (2011), “Osteoblast and monocyte responses to 444 ferritic stainless steel intended for a Magneto-Mechanically Actuated Fibrous Scaffold”, *Biomater.*, **32**(29), 6883-6892.
- Markaki, A.E. and Clyne, T.W. (2004), “Magneto-mechanical stimulation of bone growth in a bonded array of ferromagnetic fibres”, *Biomater.*, **25**(19), 4805-4815.

- Markaki, A.E. and Clyne, T.W. (2005), "Magneto-mechanical actuation of bonded ferromagnetic fibre arrays", *Acta Materialia*, **53**(3), 877-889.
- Markaki, A.E. and Justin, A.W. (2014), "A magneto-active scaffold for stimulation of bone growth", *Mater. Sci. Technol.*, **30**(13A), 1590-1597.
- Mosesson, M.W. (2005), "Fibrinogen and fibrin structure and functions", *J. Thrombos. Haemostas.*, **3**(8), 1894-1904.
- Mosesson, M.W., Siebenlist, K.R. and Meh, D.A. (2001), "The structure and biological features of fibrinogen and fibrin", *Ann. NY. Academy Sci.*, **936**(1), 11-30.
- Neelakantan, S., Bosbach, W., Woodhouse, J. and Markaki, A.E. (2014), "Characterization and deformation response of orthotropic fibre networks with auxetic out-of-plane behaviour", *Acta Materialia*, **66**, 326-339.
- Nilsson, K.G., Henricson, A., Norgren, B. and Dalén, T. (2006), "Uncemented HA-coated implant is the optimum fixation for TKA in the young patient", *Clinic. Orthop. Relat. Res.*, **448**, 129-139.
- Pittenger, M.F., Mackay, A.M., Beck, S.C., Jaiswal, R.K., Douglas, R., Mosca, J.D., Moorman, M.A., Simonetti, D.W., Craig, S. and Marshak, D.R. (1999), "Multilineage potential of adult human mesenchymal stem cells", *Sci.*, **284**(5411), 143-147.
- Silverman, R.P., Passaretti, D., Huang, W., Randolph, M.A. and Yaremchuk, M. (1999), "Injectable tissue-engineered cartilage using a fibrin glue polymer", *Plastic Reconstruct. Surg.*, **103**(7), 1809-1818.
- Spear, R.L., Symeonidou, A., Brooks, R.A. and Markaki, A.E. (2015), "In vitro assessment of porous magneto-active coatings for implant osseointegration", *Reference Module in Materials Science and Materials Engineering*, S. Hashmi, Elsevier, in press.
- Spear, R.L., Brooks, R.A. and Markaki, A.E. (2013), "Short-term in vitro responses of human peripheral blood monocytes to ferritic stainless steel fiber networks", *J. Biomed. Mater. Res. Part A*, **101**(5), 1456-1463.
- Spear, R.L., Strigengan, B., Neelakantan, S., Bosbach, W., Brooks, R.A. and Markaki, A.E. (2015), "Physical and biological characterization of ferromagnetic fiber networks: effect of fibrin deposition on short-term in vitro responses of human osteoblasts", *Tissue Eng. Part A*, **21**(3-4), 463-474.
- Symeonidou, A., Spear, R.L., Brooks, R.A. and Markaki, A.E. (2013), "Human mesenchymal stem cell response to 444 ferritic stainless steel networks", *MRS Online Proceedings Library*, **1569**, 73-78.
- Vavken, P., Joshi, S.M. and Murray, M.M. (2011), "Fibrin concentration affects ACL fibroblast proliferation and collagen synthesis", *Knee*, **18**(1), 42-46.
- Wong, C., Inman, E., Spaethe, R. and Helgersson, S. (2003), "Fibrin-based biomaterials to deliver human growth factors", *Thrombos. Haemostas.*, **89**(3), 573-582.
- Yamada, Y., Boo, J.S., Ozawa, R., Nagsaka, T., Okazaki, Y., Hata, K. and Ueda, M. (2003), "Bone regeneration following injection of mesenchymal stem cells and fibrin glue with a biodegradable scaffold", *J. Cranio-Maxillofacial Surg.*, **31**(1), 27-33.
- Zaher, W., Harkness, L., Jafari, A. and Kassem, M. (2014), "An update of human mesenchymal stem cell biology and their clinical uses", *Archive Toxicol.*, **88**(5), 1069-1082.